J Appl Electrochem (2010) 40:233–239
DOI 10.1007/s10800-009-9996-x

ORIGINAL PAPER

Electrodeposition of copper from spent Li-ion batteries by electrochemical quartz crystal microbalance and impedance spectroscopy techniques

V. G. Celante · M. B. J. G. Freitas

Received: 1 April 2009 / Accepted: 16 August 2009 / Published online: 4 September 2009

Abstract Information about the copper electrodeposition mechanism at different pH values was obtained using an electrochemical quartz crystal microbalance (EQCM) technique, as well as potentiodynamic, potentiostatic, and electrochemical impedance spectroscopy (EIS) techniques. In agreement with the measurements obtained from the EQCM and potentiostatic experiments, an intermediate Cu^{+} species and a CuO layer are formed. Simultaneous mechanism of direct reduction of Cu^{2+} and copper oxide (CuO) reduction at pH 2.0 and 4.5 occur. The EIS experiment shows a diffusion-controlled process by the presence of a Warburg element, a CPE related to the irregular metallic copper electrodeposition, and a resistance of the electrodeposit.

Keywords Copper · Li-ion batteries · Electrochemistry quartz crystal microbalance · Electrochemical impedance spectroscopy

1 Introduction

Li-ion batteries are currently gaining good market participation due to having a higher power density than either Ni–Cd or Ni–MH batteries [1]. Between 2000 and 2008, the annual production of these batteries increased by 800% and it is predicted to increase even more next years [2]. The composition of Li-ion batteries presents the cathode formed by $LiCoO_2$ on a current collector of aluminum. The electrolyte of these batteries is an inorganic salt of Li dissolved in a solvent or a mixture of organic solvents. The anode is usually formed by carbon materials on a current collector composed of copper [3]. Li-ion battery recycling has great importance for environmental protection; however, economic factors should also be considered. In the USA, Japan, France, Germany, and Sweden, battery recycling is a successful practice. For these regions, it is useful to study the established recycling processes of Li-ion batteries [4]. The spent batteries can be recycled by pyrometallurgical or hydrometallurgical processes. The pyrometallurgical process is undesirable due to the emission of toxic gases into the environment. The hydrometallurgical process is thus more favorable from an environmental conservation viewpoint. In the hydrometallurgical process, after battery dismantling occurs, the electrodes are dissolved in concentrated acids. After this stage, the metal ions in the resultant solution can be recovered by one of three methods: precipitation, extraction, or electrodeposition. Electrochemical recycling is a viable process for the production of copper metallic films, alloys, and multilayer deposits with controlled structure and morphology. For this reason, part of copper electrochemical recycling is the study of its electrodeposition mechanism. To study electrochemical recycling, it is necessary to analyze the mechanism of copper electrodeposition at different solution pHs. The production of metallic copper is accomplished predominantly via electrodeposition in aqueous solution [5].

The EQCM technique is very effective in the study of the mechanism of metal electrodeposition for thin films. In EQCM technique, the mass variation is calculated by the Sauerbrey equation (Eq. 1),

$$\Delta f = \left(\frac{-2f_0^2\Delta m}{A\sqrt{\mu_i\rho_i}}\right) = -\Delta m K, \quad (1)$$

V. G. Celante · M. B. J. G. Freitas (✉)
Universidade Federal do Espírito Santo, Av. Fernando Ferrari 514, Goiabeiras, Vitória, ES 29075-910, Brazil
e-mail: marcosbj@hotmail.com; marcosbj@gmail.com

where f_0 is the resonance frequency of the quartz crystal, A is the piezoelectric active area, μ_i is the quartz shear modulus, K is the experimental mass coefficient, and ρ_i is the density of quartz.

Some authors [5–8] have studied electrodeposition performed with the aid of the EQCM and have also observed that, in acidic solutions, copper electrodeposition can be performed by direct deposition (DD), which is related to the direct reduction of Cu^{2+} to Cu, as seen in Eq. 2:

$$Cu^{2+}_{(aq)} + 2e^- \rightarrow Cu_{(s)} \quad (2)$$

The theoretical mass/charge (m/z) value for reaction (2) is equal to 31.81 g mol^{-1} ($M^{2+}_{Cu}/2e^-$).

Copper electrodeposition can be performed by a two-step deposition, from Cu^{2+} to Cu^+ and then to Cu, as seen in Eqs. 3 and 4. The theoretical m/z values for reactions (3) and (4) are both equal to 63.6 g mol^{-1} ($M^{n+}_{Cu}/1e^-$).

$$Cu^{2+}_{(aq)} + e^- \rightarrow Cu^{+}_{(aq)} \quad (3)$$

$$Cu^{+}_{(aq)} + e^- \rightarrow Cu^{+}_{(s)} \quad (4)$$

In the copper electrodeposition process, the interface electrode solution becomes alkaline due to water reduction. The local alkalization that occurs in the interface electrode solution can provoke the precipitation of CuO and Cu_2O, as shown in the Pourbaix diagram for copper in an aqueous system (Fig. 1). Copper electrodeposition can be performed by the reduction of copper oxide with an increase in pH at the interface, as seen in Eqs. 5 and 6.

$$Cu_{(s)} + 2H_2O_{(l)} \rightarrow Cu^{2+}_{(aq)} + H_{2(g)} + 2OH^-_{(aq)} + 4e^- \quad (5)$$

$$2Cu^{2+}_{(aq)} + H_2O_{(l)} + 2e^- \rightarrow Cu_2O_{(s)} + H_2O^+_{(aq)} \quad (6)$$

Gabás and Bijani [9] studied the process of formation of thin films for nanostructural copper. The authors demonstrated that copper electrodeposition could be performed with the formation of Cu_2O layers, related to the increase in the interface pH value, in accordance with Eq. 7.

$$2Cu^{2+}_{(aq)} + 2e^- + 2OH^-_{(aq)} \rightarrow Cu_2O_{(s)} + H_2O_{(l)} \quad (7)$$

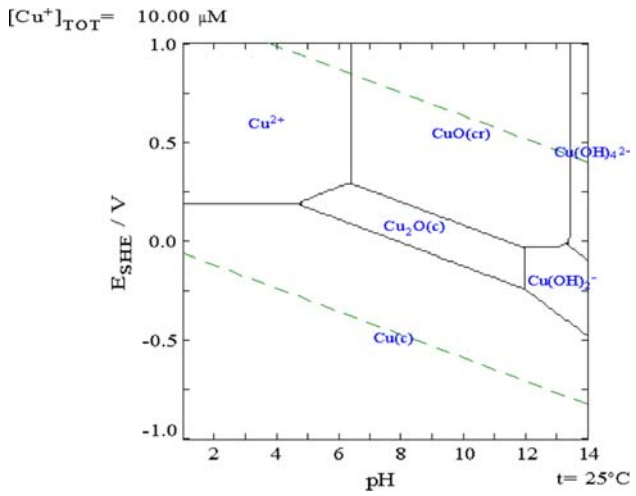

Fig. 1 Pourbaix diagram for copper in aqueous solutions

Electrochemical impedance spectroscopy (EIS) has great effectiveness in the study of interfacial processes and the characterization of porous electrodes. When used in electrochemical systems, EIS can provide information about the kinetics of electrode processes and the structure of the electric double layer. Hence, it has been employed in the study of corrosion, batteries, electrodeposition, and electro-synthesis. Previous research in copper electrodeposition found that, in EIS, the copper electrodeposits showed two interfaces: one related to a metallic copper layer and another to an oxide layer, normally Cu_2O [8, 10–12].

In this study, the EQCM technique was used together with impedance spectroscopy, and potentiodynamic and potentiostatic techniques to obtain information about the electrodeposition mechanism for copper from the anodes of spent Li-ion batteries.

2 Experimental procedure

2.1 Preparation of electrodeposition solutions

Spent Li-ion batteries were physically dismantled and separated into their different parts: anode, cathode, organic separators, steel compartment, and current collectors. The negative electrode (copper + carbon material) was separated. This material was dried in air at 120 °C for 24 h to evaporate organic compounds present in the electrolyte solution, such as ethylene carbonate and propylene carbonate. The current collector was also separated from the active material. The copper current collector was then washed with distilled water at 40 °C to eliminate lithium salts also present in the electrolyte. A mass of 9.21 g of current collector was dissolved in a solution containing 470.00 mL of 3.00 mol L^{-1} H_2SO_4, and 30.00 mL of 30% v/v H_2O_2, and the system was kept under magnetic stirring at 60 °C for 2 h. The addition of H_2O_2 is necessary to increase the efficiency of copper dissolution, since copper is partially insoluble in H_2SO_4 solutions. The carbon active material was separated by filtration from the leaching solution. All experimental procedures can be seen in Fig. 2. Equation 8 shows the entire process:

$$Cu_{(s)} + H_2SO_{4(aq)} + H_2O_{2(aq)} \rightarrow CuSO_{4(aq)} + 2H_2O_{(l)} \quad (8)$$

The pH of the leaching solution was adjusted with KOH pellets to 2.0 or 4.5. The solutions were buffered with 0.10 mol L^{-1} H_3BO_3, and 0.5 mol L^{-1} K_2SO_4 was added

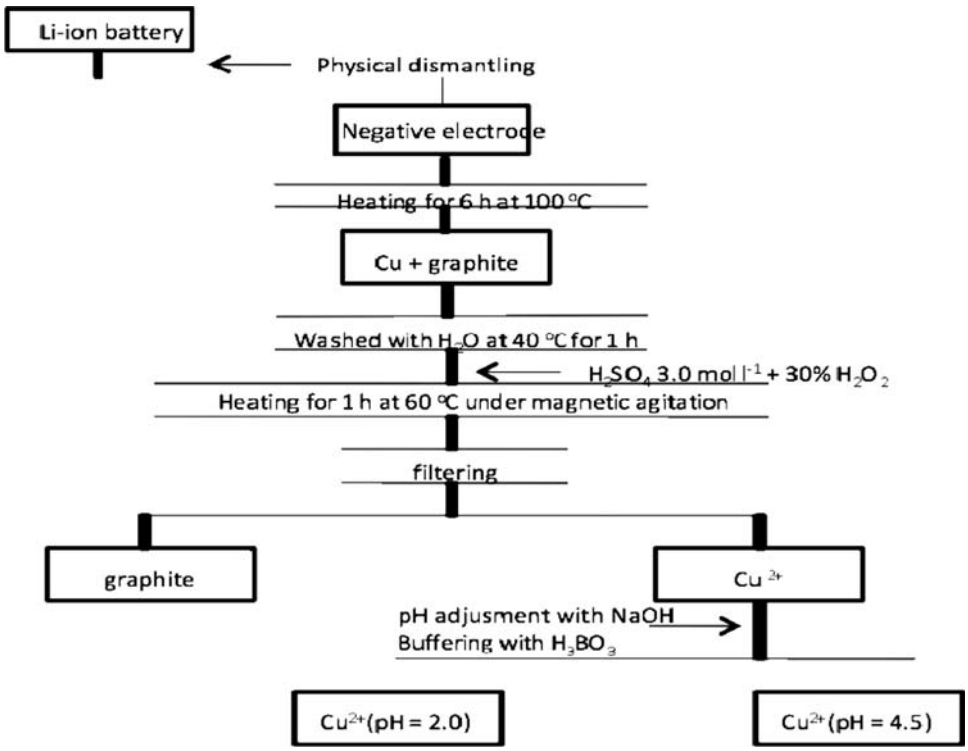

Fig. 2 Experimental procedure scheme for the preparation of copper solutions

as a supporting electrolyte. The ionic copper concentration in the baths was equal to 0.00098 mol L^{-1}, as measured by inductively coupled plasma mass spectroscopy. The copper solution was submitted to a nitrogen flux for 30 min to eliminate the presence of oxygen.

2.2 Electrochemical measurements

Potentiostatic and EQCM studies were performed in an E.G & G PAR 263A with a SEIKO QC A917 frequencimeter. The fundamental frequency of the quartz crystal was 8.996 MHz (SEIKO). The working and auxiliary electrodes were made of platinum and the reference electrode was Ag/AgCl/KCl saturated. Potentiostatic experiments were performed by applying potentials of −0.20, −0.30, and −0.40 V for 30 s for copper reduction. Potentiodynamic experiments were performed with an initial potential range of 0.00 to −0.80 V, a reverse scan to +1.00 V, and a return to the initial potential. The scan rate was equal to 20.00 mV s^{-1}. EIS was performed in an AUTOLAB PGSTAT 100 with an EIS module, in the frequency range of 1.0 MHz to 0.1 mHz with an amplitude of 10 mV in 0.5 mol L^{-1} H_2SO_4 to avoid possible copper spontaneous deposition. The working electrode was Pt (0.07 cm^2). The counter electrode was made of graphite (3.00 cm^2) and the reference electrode was Ag/AgCl/KCl saturated.

3 Results and discussion

3.1 Potentiostatic and EQCM measurements

Figure 3a shows the voltammogram for copper electrodeposition at pH 2.0. After an applied potential of −0.3 V, the current density remained constant until reaching a potential of −0.5 V. The non-dependence between the current and the potential observed in Fig. 3a can be attributed to a diffusion-controlled process or to copper oxide film formation. For the dissolution process, in the range of +0.6 to +0.8 V, the results show two regions due to the formation of an intermediary Cu^+ compound, and the formation of a copper oxide. The voltammogram curve obtained for copper electrodeposition at pH 4.5 presents similar behavior (Fig. 3b). In this case, two peaks can be seen at −0.4 and −0.5 V, due to the reduction of Cu^{2+} to Cu^+ and Cu. At potentials from −0.5 to −0.75 V, the current density remained constant. This behavior can be attributed to a diffusion-controlled process or to copper oxide film formation. Again, in the anodic region, there are two peaks for dissolution, suggesting a two-step process for dissolution of this electrodeposit.

Potentiostatic and EQCM measurements were performed. Figure 4a, b shows typical chronoamperometric plots for Cu^{2+} electrodeposition in acidic solution. In the copper electrodeposition, a transient current was observed as soon as the potential was turned on. The transient

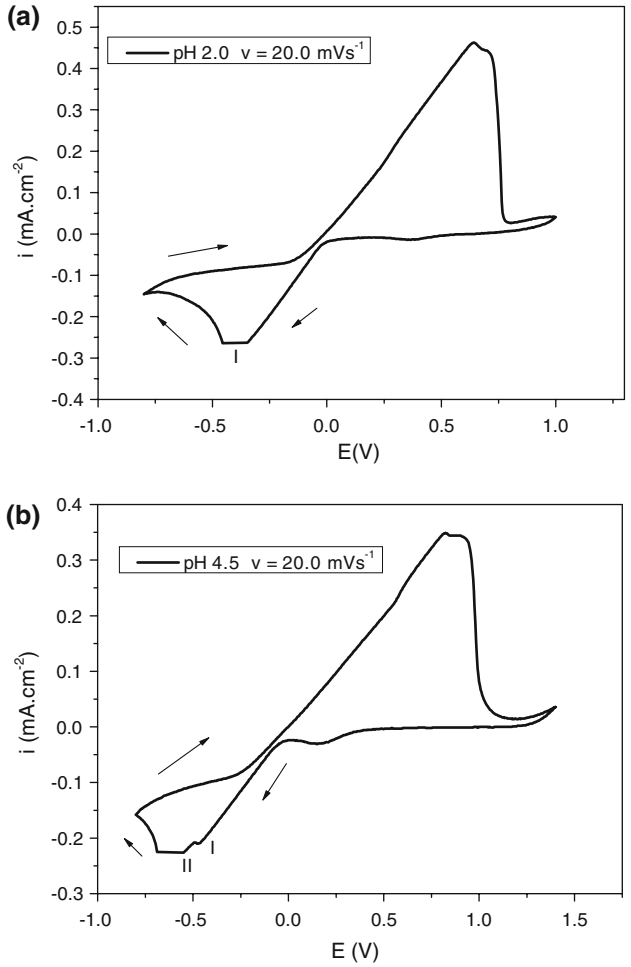

Fig. 3 Cyclic voltammogram curves obtained at a copper concentration of 0.001 mol L^{-1}, with 2.7, H_3BO_3 0.10 mol L^{-1} as buffer. The potential scan rate was 20.00 mV s^{-1}, **a** pH = 2.0, **b** pH = 4.5

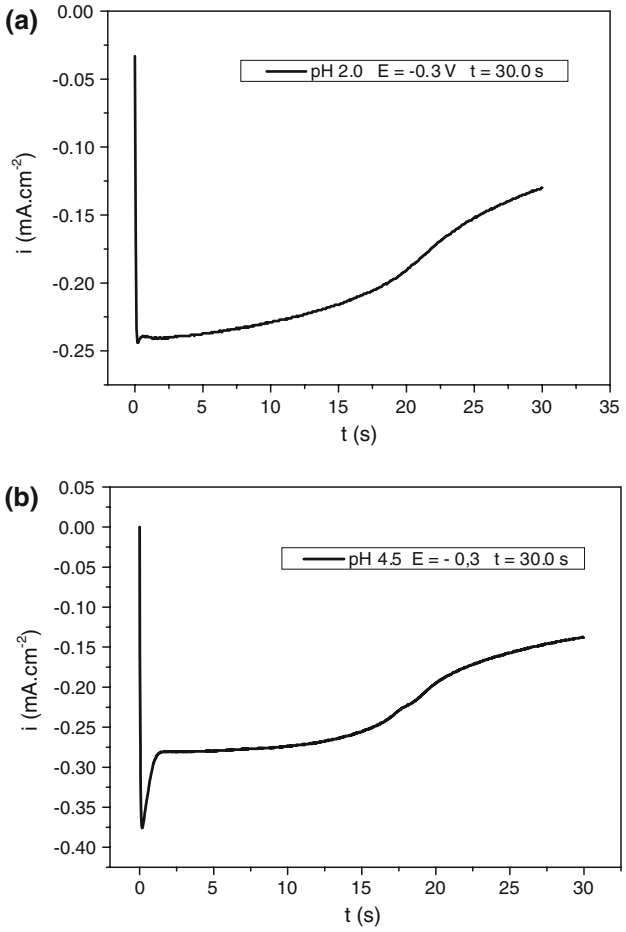

Fig. 4 Chronopotentiometry for copper electrodeposition at $E = -0.3$ V with $[Cu^{2+}] = 0.001$ mol L^{-1}, $t = 30$ s and H_3BO_3 as a buffer at **a** pH = 2.0, **b** pH = 4.5

current density reaches its maximum value, due to the nucleation and growth of the electrodeposit. The current density decreased with the increase in deposit surface area. As a result, the current led to lower cathodic values with increasing electrodeposition time [13].

The variations of *m/z* as functions of time for the chronoamperogram plots are shown in Fig. 5. Experimental *m/z* values were compared with theoretical values obtained for mechanisms of more probable reactions. The *m/z* values for this process, as seen in Fig. 5a, b, show the presence of Cu^+ species (63.03 g mol^{-1}) in an initial stage, quickly turning to DD. In Fig. 5a, b, the presence of a *m/z* values equals to 39.05 and 39.55 g mol^{-1}, respectively, is an indicative of the presence of a CuO layer close to the value of the theoretical *m/z* (39.75 g mol^{-1}). As shown in Fig. 5, it was observed that experimental *m/z* values obtained during copper electrodeposition in solutions at pH 2.0 and 4.5 moved toward a value of 36.00 g mol^{-1} as the deposition advanced. This result suggests that deposition is occurring in agreement with the mechanism of DD of metallic copper, as described by Eq. 2, and with an increase in pH at the interface, which leads to a reduction of the CuO layer.

The electrodeposition process that occurs with ionic copper can be analyzed in different stages. In the first stage, the reduction mechanism of the ionic copper is represented by Eqs. 3 and 4. Equations 9–11 describe the electrodeposition process through formation of a copper oxide intermediate. The DD that occurs simultaneously with copper oxide deposition, which is related to the direct reduction of Cu^{2+} to Cu, is represented by Eq. 2.

$$2H_2O_{(l)} + 2e^- \rightarrow H_{2(g)} + 2OH^-_{(aq)} \quad (9)$$

$$Cu^{2+}_{(aq)} + 2OH^-_{(aq)} \rightarrow CuO_{(s)} + H_2O_{(l)} \quad (10)$$

$$CuO_{(s)} + 2H^+_{(aq)} + 2e^- \rightarrow Cu_{(s)} + H_2O_{(l)} \quad (11)$$

EQCM curves for copper electrodissolution at both pH values were made to explain the anodic peaks observed in the voltammogram (Fig. 2), which is shown in Fig. 6a, b. The

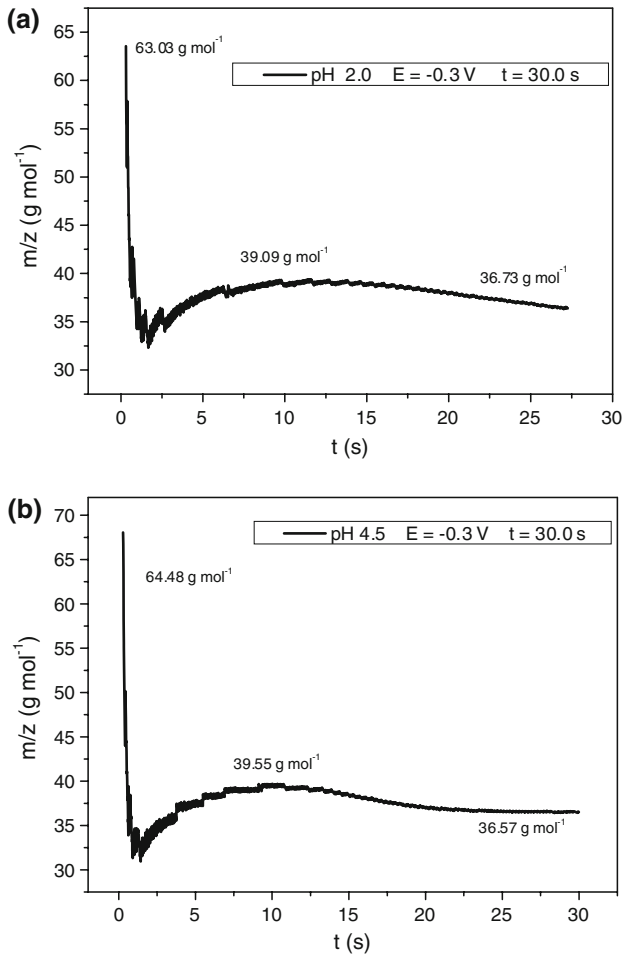

Fig. 5 EQCM results for copper electrodeposition with $[Cu^{2+}] = 0.001$ mol L^{-1}, with $v = 20$ mV s^{-1} and H_3BO_3 as a buffer at **a** pH = 2.0, **b** pH = 4.5

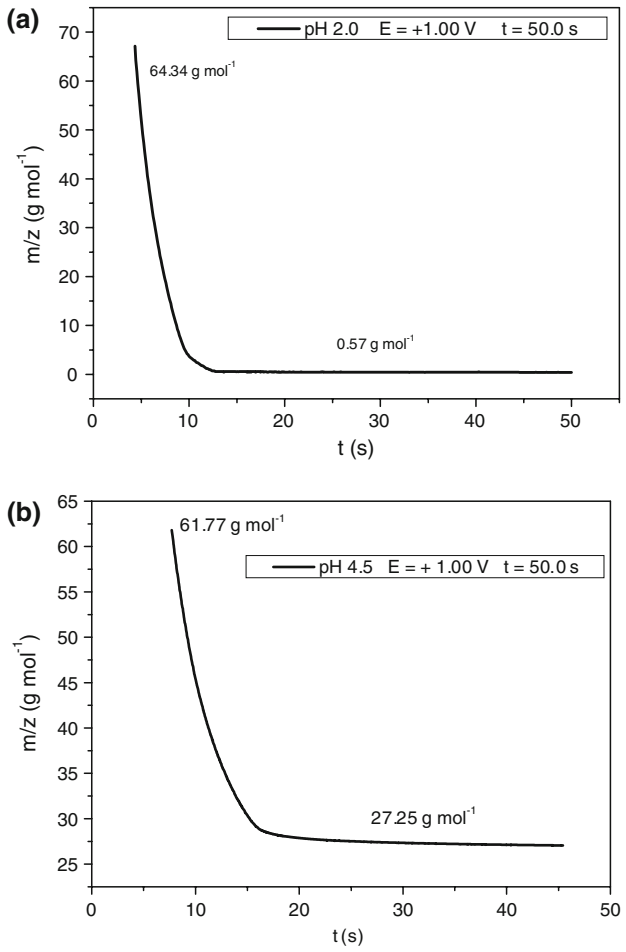

Fig. 6 Potentiostatic electrodissolution of copper deposits under $E = +1.00$ V with $[Cu^{2+}] = 0.001$ mol L^{-1}, $t = 30$ s and H_3BO_3 as a buffer at **a** pH = 2.0, **b** pH = 4.5

electrodes were polarized at +1.00 V. At pH 2.0, the *m/z* values equal to 64.34 g mol^{-1} obtained in the initial process turned to 32.21 g mol^{-1} (Fig. 6a). This result indicates that metallic Cu dissolution occurs through the formation of an intermediate Cu^{1+} in the solution. This fact can also suggest that the presence of an intermediate Cu^{+} species is fast, leading to direct dissolution [13–15]. At pH 4.5, the *m/z* value encountered was 61.67 g mol^{-1} for as long as electrodissolution was performed (Fig. 6b). This value was equal to 27.25 g mol^{-1} in the final steps. The copper deposited is not totally dissolved. This indicates that at pH 4.5 the copper oxide layer is a more resistive electrodeposit than at pH 2.0. Experimental *m/z* values were lower than the theoretical values owing to the oxygen reaction, which decreases the efficiency for copper electrodissolution.

3.2 EIS measurements

The Nyquist and Bode plots of the EIS experiments for copper electrodeposited at pH 2.0 (Fig. 7a) and 4.5 (Fig. 7b) onto a Pt working electrode (0.07 cm^2) are shown in Fig. 7. The open-circuit potential (E_{oc}) at which the experiment was performed was equal to 0.020 V (pH = 2.0) and 0.019 V (pH = 4.5). A semi-circle aspect is first observed in the Nyquist plot, followed by a straight line whose tangent to the real axis is 45°. The straight line whose tangent to the real axis is 45° is related to a Warburg diffusion process. From the Bode Plot, it can be seen that the phase angles change slightly with frequency, and that no characteristic frequency can be identified in the 1.0–10 Hz interval at pH 2.0 or the 0.10–1.0 Hz interval at pH 4.5. This is a characteristic of the capacitance dispersions represented by the constant phase element (CPE). The CPE is related to the irregular metallic copper electrodeposition. This process occurs by the change in electrode surface, where nuclei are formed and deposits appear in a non-homogeneous form. When the kinetic process is not the determinant in the electrodeposition process, Warburg impedance occurs, leading to a diffusion process [16, 17]. Warburg impedance represents the diffusion of H^{+} ions

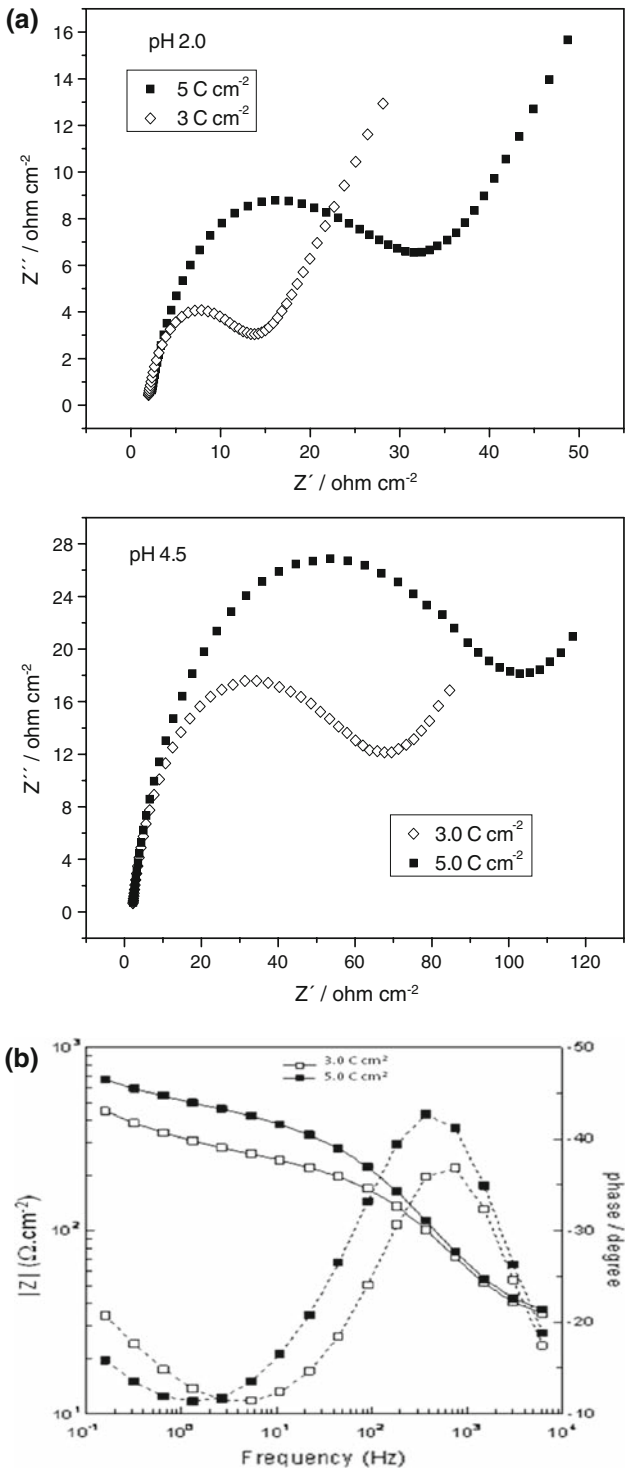

Fig. 7 Nyquist and Bode plots for copper electrodeposition with an amplitude of 10 mV and a frequency range of 1.0 MHz to 0.1 mHz on a Pt substrate (0.07 cm^2). **a** pH = 2.0, **b** pH = 4.5

from the electrolyte to the pores of copper and the copper oxide porous layer.

The simulation of the circuit performed in FRA software can be seen in Fig. 8, where R_s is the solution resistance, R_p is the polarization resistance, Q is the CPE, and W is the Warburg impedance.

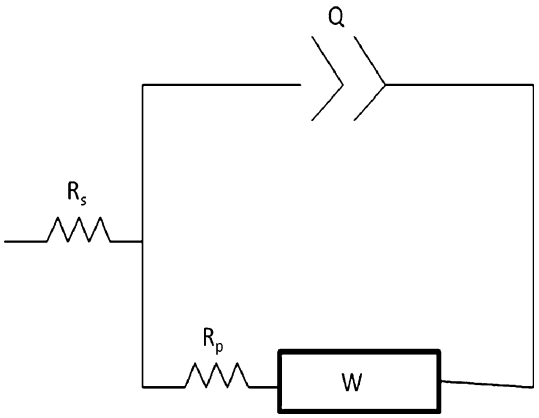

Fig. 8 Equivalent circuit for copper electrodeposition in the EIS experiment

Tables 1 and 2 show the circuit element values associated with the electrodeposition of copper at pH 2.0 and 4.5. Table 1 shows the circuit element values for copper electrodeposited onto Pt at an applied charge density of 3.0 C cm^{-2} in both pH cases. The value of the polarization resistance (R_p) is higher for copper electrodeposited at pH 4.5 than at pH 2.0. The increase in the polarization resistance at pH 4.5 occurs due to the formation a resistive layer of CuO. The EIS are totally compatible with the EQCM measurements (Fig. 6). By monitoring the increase in

Table 1 Circuit-element values of EIS of copper electrodeposition for $q = 3.0$ C cm^{-2}, at pH = 2.0 and 4.5

Element	pH = 2.0		pH = 4.5	
	Value	Error (%)	Value	Error (%)
R_s (Ω cm^{-2})	1.82	6.03	1.555	8.41
R_p (Ω cm^{-2})	12.4	6.08	104.3	3.09
Q (μF)^n	3.94×10^{-4}	11.1	6.09×10^{-4}	9.40
n	0.7834	2.77	0.678	2.03
$W_o - R$	29.9	12.1	31.1	3.21

Table 2 Circuit-element values of EIS experiment of copper electrodeposition for $q = 5.0$ C cm^{-2}, at pH = 2.0 and 4.5

Element	pH = 2.0		pH = 4.5	
	Value	Error (%)	Value	Error (%)
R_s (Ω cm^{-2})	1.909	6.483	1.554	8.825
R_p (Ω cm^{-2})	23.89	10.512	60.25	3.120
Q (μF)^n	0.0004506	12.109	0.0008372	11.278
n	0.75367	3.7011	0.65473	2.5131
$W_o - R$	42.15	7.1329	45.12	7.996

charge density from 3.0 to 5.0 C cm^{-2}, and maintaining a constant pH at 2.0, we have verified that the polarization resistance increases due to the increase in the CuO layer. This result was also expected at pH 4.5. However, with the increase in charge density, the R_p value decreases (104.3–60.25 C cm^{-2}). The decrease in the polarization resistance is indicative that a more porous electrodeposit is formed at pH 4.5 with the increase in the charge density. The n values do not approach those of an ideal capacitor (1.0). This deviation is related to a heterogeneous surface [8, 18, 19]. The EIS resulted in measurements compatible with those obtained from the potentiodynamic and EQCM experiments.

4 Conclusions

Using an EQCM, we have verified the mechanism for copper electrodeposition and correlated it with solution pH, electrochemical conditions, and EIS. EQCM and potentiostatic experiments show that the intermediate Cu^+ and a CuO layer are present in the mechanism of copper electrodeposition. Copper potentiostatic electrodeposition at pH 2.0 and 4.5 occurs via simultaneous mechanisms of direct reduction and copper oxide reduction. The potentiostatic dissolution of copper shows that, at pH 2.0, almost 100% of the electrodeposit was dissolved, and whereas at pH 4.5, there is a resistive layer of CuO that does not dissolve. EIS experiments show a diffusion-controlled process by the presence of a Warburg element, a CPE related to the irregular metallic copper electrodeposition, and a resistive CuO layer.

Acknowledgment The authors acknowledge MCT-CNPq-FAPES process number 36303542/2007 for its financial support.

References

1. Takeno K, Takano K, Ichimura M et al (2005) J Power Sources 142:298–305
2. Hawkins M (2007) 2006 production statistics. In: Cobalt News. Cobalt Development Institute. Available via articles. http://www.thecdi.com/cdi/images/news_pdf/Cobalt_News_Apr07.pdf. Accessed 14 Apr 2007
3. Jovic VD, Jovic BM (2001) J Serb Chem 66:935–952
4. Majidi MR, Asadpour-Zeynali K, Hafezi (2009) Electrochim Acta 54:1119–1126
5. Pasquale MA, Gassa LM, Arvia AJ (2008) Electrochim Acta 53:5891–5904
6. Gabrielli C, Devos O, Beitone L et al (2007) J Electroanal Chem 606:95–102
7. Schneider O, Matic S, Argirusis C (2008) Electrochim Acta 53:5485–5495
8. Zangari G, Arrington D, Curry M et al (2008) Electrochim Acta 53:2644–2649
9. Gabás M, Bijani S (2007) Thin Solid Films 515:5505–5511
10. Savadogo O, Fricoteaux P (1999) Electrochim Acta 44: 2927–2940
11. Johnson WB, Macdonald JR (2005) In: Barsoukov E, Macdonald JR (eds) Impedance spectroscopy theory: experiment and applications, 2nd edn. Willey, New York
12. Cavallotti PL, Vincenzo A (2002) J Appl Electrochem 32: 743–753
13. Pesic B, Grujicic D (2002) Electrochim Acta 47:2901–2912
14. Silva MLP, Carvalho AT, Lima RR et al (2008) Sens Actuators B 130:141–149
15. Kálman E, Szõcs E, Vastag G et al (2005) Corros Sci 47:893–908
16. Machado SAS, Miwa DW et al (2006) J Braz Chem Soc 17:1339–1346
17. Gabrielli C, Moçotéguy P (2008) J Appl Electrochem 38:457–468
18. Kim JJ, Kang MS, Kim K et al (2008) Thin Solid Films 516:3761–3766
19. Milosev I, Kosec T (2008) Corros Sci 50:1987–1997